SATELLITE FORMATION FLIGHT RESULTS FROM PHASE 1 OF THE MAGNETOSPHERIC MULTISCALE MISSION

Trevor Williams[*], Neil Ottenstein[+], Eric Palmer[+] and Dominic Godine[+]

This paper describes the underlying dynamics of formation flying in a high-eccentricity orbit such as that of the Magnetospheric Multiscale mission. The GPS-based results used for MMS navigation are summarized, as well as the procedures that are used to design the maneuvers used to place the spacecraft into a tetrahedron formation and then maintain it. The details of how to carry out these maneuvers are then discussed. Finally, the numerical results that have been obtained concerning formation flying for the MMS mission to date (e.g. tetrahedron sizes flown, maneuver execution error, fuel usage, etc.) are presented in detail.

INTRODUCTION

The NASA Magnetospheric Multiscale (MMS) mission is flying four spinning spacecraft in highly elliptical orbits to study the magnetosphere of the Earth[1]. MMS was launched on an Atlas V 421 from Kennedy Space Center on Mar. 12, 2015, with insertion into a high-eccentricity orbit that was designed to satisfy a complicated set of science and engineering constraints[2]. After roughly 5 months of commissioning, the spacecraft have flown in tetrahedron formations of varying dimensions in order to collect magnetospheric science measurements. In Phase 1 of the mission, when the MMS orbit had an apogee radius of 12 Earth radii, these measurements were taken on the dayside of the Earth in a Region of Interest surrounding MMS apogee. The goal during Phase 1 was to observe the magnetospheric reconnection events that were expected to occur near the bow shock where the solar wind impinges upon the magnetosphere. Measurements during the later Phase 2b, after apogee radius has been increased during Phase 2a to 25 Earth radii, will be taken in the magnetotail[3], to similarly observe nightside magnetic reconnection events. Taking simultaneous measurements from four spacecraft allows spatial derivatives of the electric and magnetic fields to be determined, allowing variations that are functions of distance to be distinguished from those that are functions of time.

This paper describes the results that have been obtained to date concerning MMS formation flying, updating the results presented in Reference 4. The MMS spacecraft spin at a rate of 3.05 RPM, with spin axis roughly aligned with Ecliptic North. Several booms are used to deploy instruments: two 5 m magnetometer booms in the spin plane, two rigid booms of length 12.5 m along the positive and negative spin axes, and four flexible wire booms of length 60 m in the spin plane. Minimizing flexible motion of the wire booms requires that reorientation of the spacecraft spin axis be kept to a minimum: this is limited to attitude maneuvers to counteract the effects of gravity-gradient and apparent solar motion. Orbital maneuvers must therefore be carried out in essentially the nominal science attitude. These burns make use of a set of monopropellant hydrazine thrusters: two (of thrust 4.5 N) along the spin axis in each direction, and eight (of thrust 18 N) in the spin plane; the latter are pulsed at the spin rate to produce a net Δv. The on-board accelerometer-based Delta-V controller[5] is used to accurately generate a commanded Δv. Navigation makes use of a weak-signal GPS-based system[6]: this allows signals to be received even when MMS is flying above the GPS orbits, producing a highly accurate determination of the four MMS orbits. This data is downlinked to the MMS Mission Operations Center (MOC) and used by the MOC Flight Dynamics Operations Area (FDOA) for maneuver design. These commands are then uplinked to

[*] Aerospace Engineer, Navigation and Mission Design Branch, NASA Goddard Space Flight Center, Greenbelt, MD 20771. Phone: (443)545-4736. Email: Trevor.W.Williams@nasa.gov

[+] Aerospace Engineer, ai Solutions, Inc., 4500 Forbes Blvd #300, Lanham, MD 20706.

the spacecraft and executed autonomously using the controller, with the ground monitoring the burns in real time.

Reference 4 described the formation flying results that were obtained during the earliest portions of the mission, referred to as Phases 0, 1a and 1x. Subsequent to this, MMS entered into science collection during its second dayside passage, termed Phase 1b. A significant factor for this phase from the flight dynamics point of view was that the science team requested that the spacecraft be flown in as small a formation as possible: this was motivated by the science data that was collected concerning magnetic reconnection during Phase 1a. This data showed that the electron diffusion region associated with a reconnection event was typically smaller than the smallest formations (scale size 10 km) that were flown during Phase 1a. As a result, there were cases where three of the four MMSs flew through an electron diffusion region, but never all four, as would be ideal for science. However, the original mission specification for Phase 1 was that MMS be capable of flying in formation scale sizes from 10 km to 160 km; all maneuver-related systems were therefore designed with this goal in mind. It was therefore not a trivial task to be able to fly in formations smaller than 10 km. The MMS flight dynamics team consequently had to carry out extensive analysis and testing to determine the smallest safe formation scale size: this was determined to be 7 km, which was deemed fully satisfactory by the science team.

This new minimum formation size was driven predominantly by the execution errors produced by the on-board delta-v controller: if this system had not been exceeding its specifications, flying at 7 km would not have been possible. An implication of flying in smaller formations is that more frequent maneuvering is usually required. The typical interval between maneuvers for 7 km formations was in the range 2-4 weeks, whereas it had been 4-5 weeks for the larger formations. These more frequent maneuvers, often triggered by two spacecraft drifting too close together, caused a small amount of time to be lost for science, since the instruments have to be turned off when burning. However, the science team felt that this tradeoff was definitely one worth taking.

Numerical results that describe the performance of the formation maneuvers are presented in the paper, as well as details of the analysis required for the small formations. Finally, the flight dynamics team has exercised several techniques to extend the intervals between full sets of formation maintenance maneuvers in the 7 km formations: these are described also.

MMS FORMATION FLYING BACKGROUND

In order to collect the science data that is required in order to study magnetic reconnection, the MMS spacecraft must fly in a tetrahedron formation (so spanning all three axes) in the science Region of Interest (RoI) of the orbit. This region is an extended arc that contains apogee, where the radius of the orbit is in the range where reconnection is expected to occur: for the MMS Phase 1 orbit, this is all radii of 9 Earth radii (R_E) or greater. It should be noted that the orientation of the tetrahedron is not specified: any orientation will give the spread across each of the three axes that is required for science.

In order for the formation to persist over multiple orbits (referred to below as revs), it is necessary for the spacecraft to take up essentially the same relative positions from one rev to the next. If this is to occur, the four MMS orbits must have essentially equal periods. Since period is directly related to semi-major axis (SMA), the key is to have the SMAs of the four orbits be closely matched. Any differences will lead to drift rates (which can be either expanding or closing) between the spacecraft. Once the accumulated drift is sufficiently large, the tetrahedron will be distorted enough that it is no longer suitable for science data generation: maneuvers will then be required in order to reestablish a high-quality formation.

Since the MMS orbit is highly eccentric (eccentricity 0.8182 for Phase 1, 0.9084 for Phase 2b), the behavior of the formation when traveling from apogee to perigee and back is quite complicated. Consider

the along-track separation between any pair of spacecraft: this is created by setting up the appropriate difference in phasing between the satellites. For instance, suppose that an along-track spacing of 18 km is required at apogee: since orbital speed at Phase 1 apogee is approximately 0.9 km/s, this will be achieved by having one spacecraft fly 20 s ahead of the other. But the orbital speed at perigee is around 9 km/s: this same lead time will therefore result in an along-track spacing of 180 km at perigee, a tenfold increase. This "breathing mode" around the orbit implies that along-track separation in the RoI will be at its minimum at apogee, increasing somewhat in the vicinity of RoI entry and exit.

The out-of-plane (OOP) relative motion is quite different. To have a specified (and maximal) OOP spacing at apogee, the common (or node) points of the corresponding pair of MMS orbits should occur at true anomalies in the vicinity of 90 deg and 270 deg. As a result of this geometry, and since apogee radius is 10 times as large as perigee radius, the OOP spacing will be roughly 10 times greater at apogee than at perigee. Furthermore, the sign of the relative displacement changes going from apogee to perigee: the spacecraft swap from side to side. Consequently, the most likely places for close approaches to occur between a pair of MMSs are at true anomalies around 90 deg or 270 deg. Care is taken in the formation maneuver design process to ensure that this does not occur. Furthermore, if a close approach (CA) were predicted to occur, a "Dodge" maneuver has been specifically designed to push one of the CA MMS pair away from the other along-track, thus increasing the miss distance significantly. This same type of maneuver can also be employed in the event of a CA being detected between an MMS and another satellite: since these other spacecraft are typically well below the MMS orbit except around perigee, any such CA will be expected to occur for true anomalies roughly in the range of 270 deg to 90 deg. This makes the Dodge maneuver design suitable for dealing with these as well, since it is designed specifically for CAs in this true anomaly range. (See the companion paper Reference 7 for further details on how MMS deals with CAs.)

Finally, since the orbits must have the same SMAs, any radial separation between these spacecraft at apogee must be set up by introducing a small difference in eccentricity, δe: one orbit will therefore have apogee radius $a\delta e$ above the other, and perigee radius $a\delta e$ below it. The radial separation therefore changes sign when going from apogee to perigee, as for the OOP case, but the magnitude stays the same at perigee and apogee.

As a result of these effects, a tetrahedron that is suitable for science will approximate a regular tetrahedron throughout the RoI, although being slightly "squashed" at apogee. At perigee, it will be extremely elongated, no longer even remotely resembling a regular tetrahedron, and will have "flipped" in the OOP and radial directions. This complicated motion to some extent approximates a tumble, with superimposed elongation and then recompression as the formation passes from apogee to perigee and back, while the same behavior is repeated from one rev to the next. Figure 1 shows the corresponding evolution in inter-satellite ranges between the 6 MMS pairs over the orbit for one of these formations. The large spikes in ISR at perigee that are caused by the increased along-track separation can clearly be seen. The extreme elongation of the formation at perigee is clearly evident.

The Quality Factor (QF) is a dimensionless parameter, lying between 0 and 1, that quantifies how close a formation is to a regular tetrahedron of the desired size: the closer to 1, the more suitable the formation. Figure 2 shows an example of the QF over several revs, from one formation to the next: the characteristic "double hump" evident in this plot is a result of the fact, discussed previously, that the formation is somewhat compressed at apogee, leading to a lower QF value at apogee itself than shortly before or after it. It can be seen that one of the two peaks gradually builds up from one rev to the next, making the QF plot increasingly unsymmetrical: this is typical of the effect of inter-satellite drift, and eventually leads to the need to perform a new set of formation maneuvers to initialize a new tetrahedron. In addition to the instantaneous QF, Figure 2 also displays the mean quality factor per RoI (Qbar), as well as the percent RoI time with QF above 0.7 (Tq). Both values are used as single value assessments of the

formation quality over an entire RoI. Definitive values for these properties are used as part of science data evaluation and predicted values for these properties are considered when determining when an extra formation maneuver may need to be performed in order to maintain a formation with sufficient quality for science purposes.

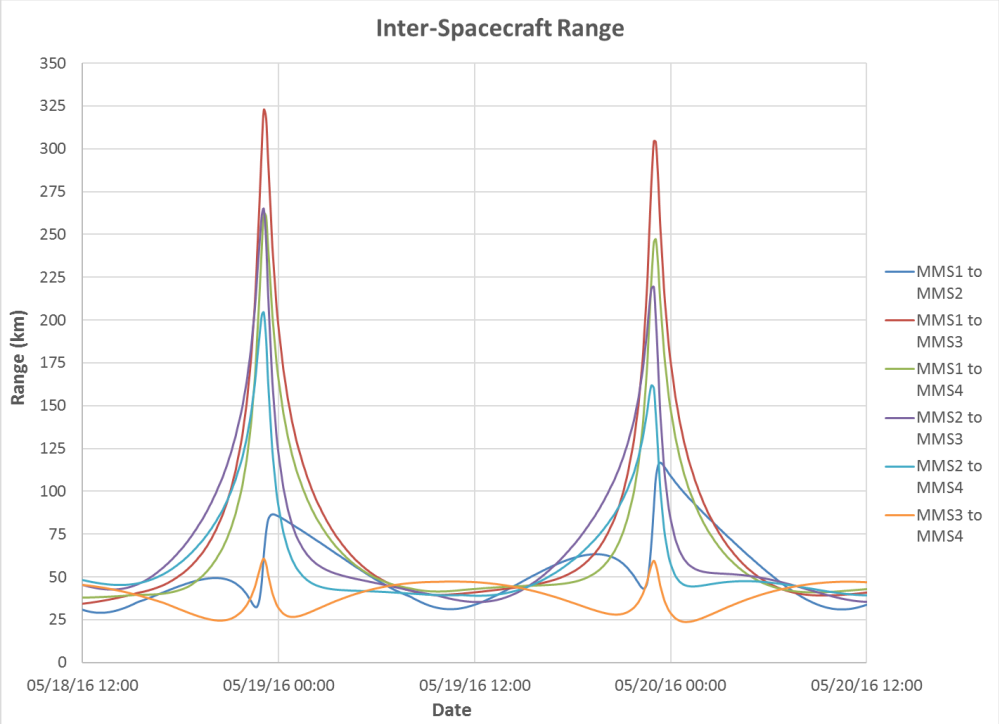

Figure 1. Six Inter-Satellite Ranges Over an Entire Orbit, 40 km Formation.

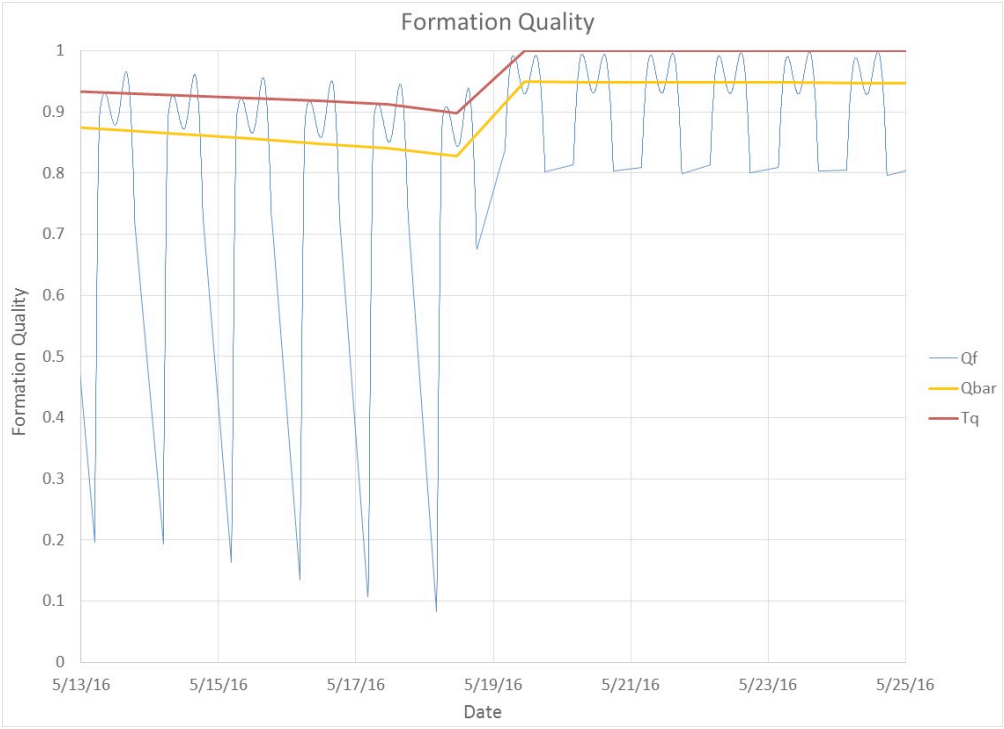

Figure 2. Quality Factor Evolution, Two 40 km Formations.

Figure 3 confirms the previous statement that the SMAs of the MMS spacecraft must be essentially equal for any viable formation. The plot covers a complete set of FM maneuvers: it can be seen that the final SMAs are indeed very nearly equal, as indeed were the SMAs before the maneuvers. Since the reference spacecraft does not maneuver, and so has a constant SMA (modulo orbital perturbations) across the FM maneuver set, it can be seen that the SMA change that is produced by the second burn of each maneuvering spacecraft must be very nearly equal and opposite to that produced by its first burn.

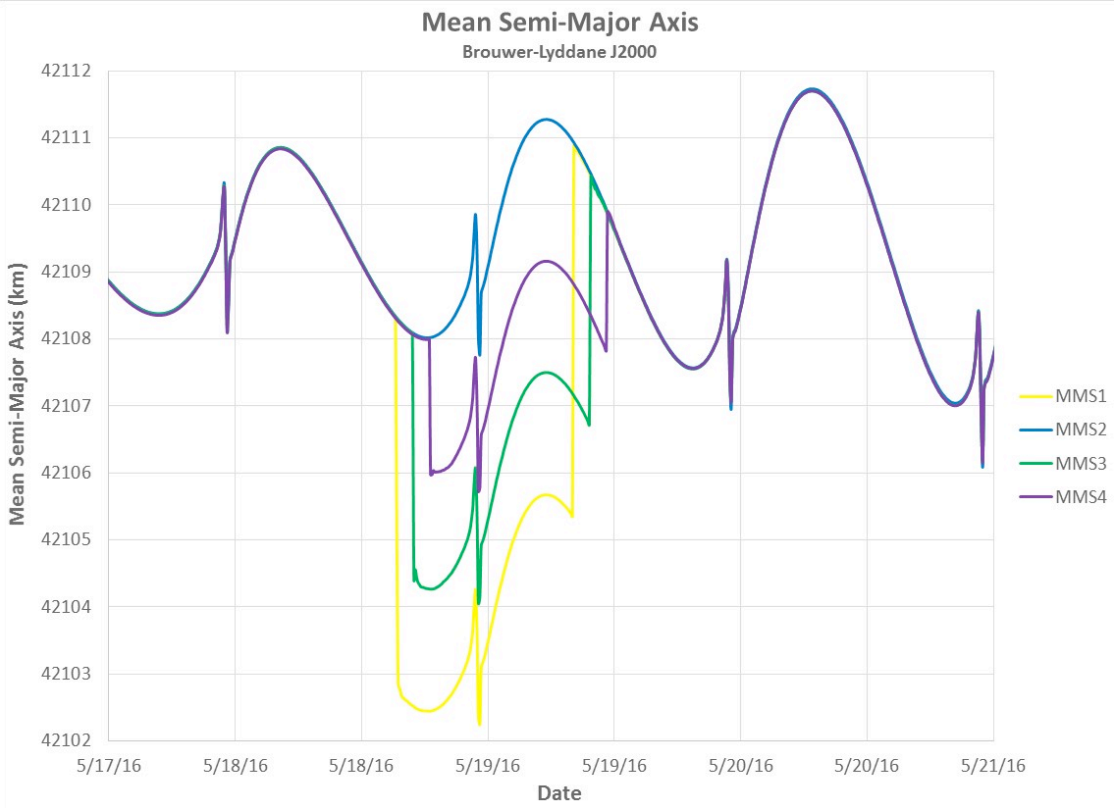

Figure 3. SMA of the Four Spacecraft Over Set of FM Maneuvers.

FORMATION MANEUVER DESIGN PROCESS

The MMS formation maneuver sequence is based on shifting the spaceraft into a fresh formation arrangement. To do so, one of the spacecraft is selected as a reference and does not performing any ΔV maneuvers. The other three spacecraft perform ΔV maneuvers so as to position themselvs into desired orbits relative to the reference spacecraft, such that all four create a tetrahedron while within the RoI. Each of the non-reference spacecraft carries out two burns: the first (FM1) on the orbit flank after apogee, and the second (FM2) in the vicinity of the subsequent apogee. This can be considered as a rendezvous pair: the first burn transfers the spacecraft from its position in the existing formation to its desired location in the new formation; the second burn then modifies its velocity so as to ensure that it continues to track the new formation geometry.

The MMS Formation Design Algorithm (FDA) (see Reference 8 for further details) designs these maneuvers by optimizing them in order to maximize the Quality Factor. Given the previous discussion on the evolution of the formation geometry throughout the RoI, it is necessary to allow a range of sizes throughout the RoI: for instance, for a 10 km formation the instantaneous mean sidelength is deemed acceptable if lying in the range of 6 to 18 km. The FDA performs a numerical optimization of the QF, subject to two key constraints: firstly, as previously noted, in order for the formation to persist, the SMAs

of the four orbits must be matched; secondly, in order to ensure safety of the spacecraft, no inter-satellite range (ISR) is allowed to go below a specified lower limit at any point on the orbit.

The orbit determination data that is used as input to the FDA is produced by the on-board Goddard Enhanced Onboard Navigation System (GEONS).[6] GEONS estimates the spacecraft's position, velocity, clock bias, clock bias rate, and clock bias acceleration using an Extended Kalman Filter (EKF) coupled with a high-fidelity dynamics model to process GPS L1 pseudorange (PR) measurements referenced to the Ultra-Stable Oscillator (USO) clock. The Navigator's weak signal acquisition capability allows the receiver to acquire and track GPS signals well above the GPS constellation and deliver highly accurate navigation solutions. The key MMS on-board orbit determination (OD) requirements were designed to ensure that the FDOA team would be able to safely and accurately maintain the range of nominal formation sizes throughout the mission. Given the extreme importance of SMA for evaluating formation persistence, the most critical requirement from GEONS is to determine SMA accurately. This is best evaluated from state data obtained after each perigee passage, when the MMS orbit passes below the GPS constellation: GEONS therefore has access to main lobe signals from typically 12 GPS satellites through perigee.

Further details of the MMS formation maneuver design and execution process are given in Reference 4.

FORMATION FLYING RESULTS THROUGHOUT PHASE 1

The MMS spacecraft performed a total of 166 maneuvers to initialize, resize, and maintain a foramation throughout the duration of Phase 1.

Table 1. Formation Initialization and Resize Maneuvers, Launch to Phase 2a.

Maneuver	Orbit	Date
Formation Initialization (160 km)	116-119	July 7-9, 2015
Formation Resize to 60 km	188-189	Sept. 16-17, 2015
Formation Resize to 25 km	202-203	Sept. 30-Oct. 1, 2015
Formation Resize to 10 km	216-217	Oct. 14-15, 2015
Formation Resize to 40 km	279-283*	Dec. 16-20, 2015
Formation Resize to 10 km	307-308	Jan. 13-14, 2016
Formation Resize to 40 km	378-379	Mar. 23-24, 2016
Formation Resize to 10 km	540-541	Sept. 1-2, 2016
Formation Resize to 7 km	554-555	Sept. 15, 2016
Formation Resize to 60 km	694-695	Feb. 1-2, 2017

Table 1 lists all of the maneuvers that changed formation size during Phase 1: these start with the Formation Initialization maneuvers that set up the first 160 km formation, together with all subsequent Formation Resizes. It also includes the subsequent 60 km formation that was flown during the first week of Phase 2a as prelude to apogee-raising.

Figure 4 shows the sizes of each of the formations (in km) that were flown during Phase 1 and the first week of Phase 2a. The dates given in the third column of Table 1 allow the various changes in target formation size to be identified readily. In this plot, formation size is quantified by the instantaneous mean of the six MMS-to-MMS sidelengths evaluated throughout each RoI. This mean varies as the spacecraft fly through the RoI, giving a band of values for each rev.

* Includes missed burn recovery sequence for MMS4: see Reference 4 for details.

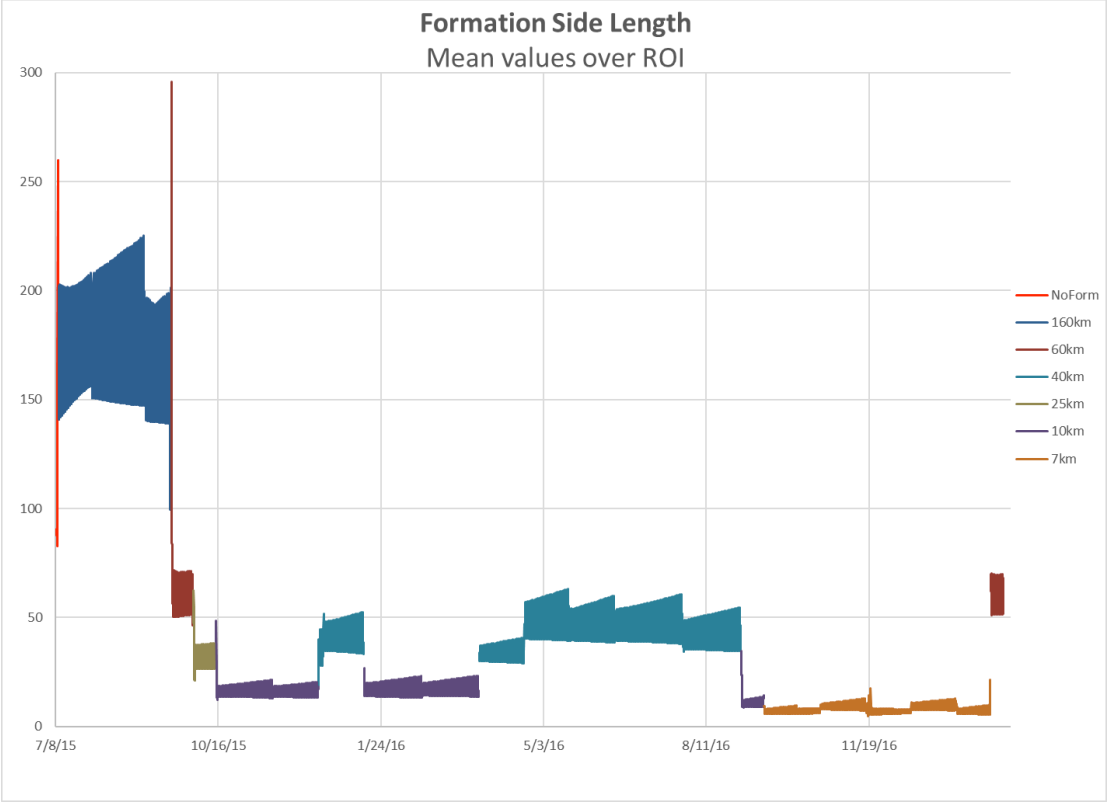

Figure 4. Evolution of Mean Sidelength, Launch to Phase 2a.

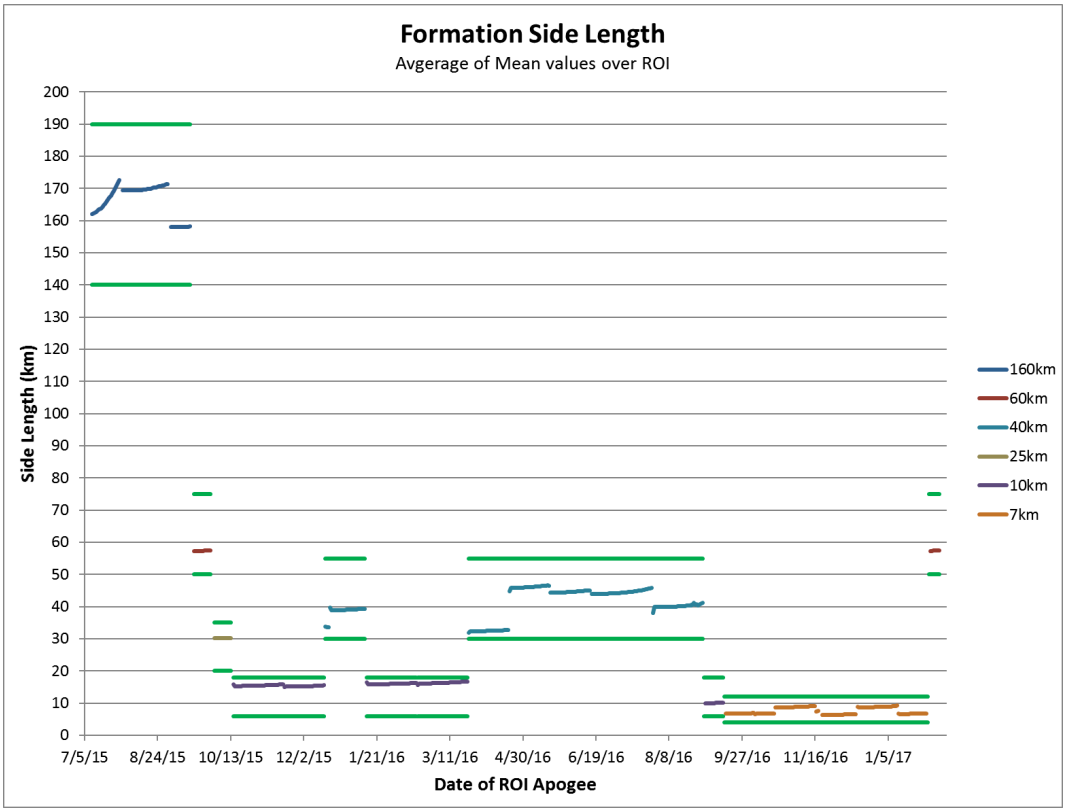

Figure 5. Evolution of Mean Sidelength Averaged Over RoI, Launch to Phase 2a.

Figure 5 then shows the corresponding average of the mean sidelengths over each RoI: this yields a single value for each rev, for simplicity. The green horizontal lines are the bounds on mean sidelength that are allowed from the definition of the QF for a target scale size. These can be thought of as the range of formation sizes that are acceptably close to the target from the point of view of science data collection. Each of the flown formations satisfied this size requirement for extended periods, typically around 3-4 weeks. An exception to this is the early formation resizes to 25 km and then 10 km: these were scheduled to occur every 2 weeks, regardless of whether the QF would have allowed longer flight at the preceding size.

The two periods that were flown at 40 km came about for very different reasons. The first arose because the science team wanted to try alternating between 10 km and 40 km formations; the second, extended period was Phase 1x, when apogee was directed away from the Sun, making this phase not conducive to collecting bowshock science data. This made the selection of formation size rather unimportant from the point of view of science. In addition, a season of long eclipses existed in this phase: power limitations prevented the spacecraft from performing maneuvers during this season. In order to ensure spacecraft safety from CAs during this non-manuevering period, the formation was spread out to 40 km.

It can be seen that the 10 km formations in late 2015 and early 2016 actually had an averaged mean sidelength of around 15 km; likewise, the preceding 25 km formation was closer to 30 km. The reason for this was the CA safety limits that are taken into account when designing formations: these tend to bias smaller formations to the upper portion of their allowable size range. While such formations clearly satisfy the science size bounds, it was desirable to try to design formations closer to the target size. This was achieved by using a much tighter set of acceptable size limits when running the FDA to generate a new formation; the original science size limits are still used when evaluating the Quality Factor to determine when maneuvers are required to reset the formation. This technique allowed a "true" 10 km formation to be generated in Sept. 2016, followed by a set of 7 km formations that were flown throughout Phase 1b in late 2016/early 2017.

Figures 6 (in km) and 7 are analogous to Figures 4 and 5, but focusing only on Phase 1b. This phase was flown almost entirely at a formation target size of 7 km: the actual averaged mean sidelength varied in a range between about 6 km and 9 km. Occasionally, the target size had to temporarily be increased to 8 km in order to obtain a viable formation solution. This arose because a difficulty that was encountered with these small formations was that the maneuvers required to set them up were sometimes quite small, which could lead to large relative execution errors as a result of the performance of the on-board Delta-V controller. Examination of Figures 8 and 9 (taken from Reference 4) shows the comparatively large errors in both magnitude and direction that can arise for the smallest maneuver sizes. It should be noted that the Delta-V controller has performed extremely well on orbit, greatly exceeding its performance specifications for even small burns. However, when flying in small formations, with their sensitivity to the drifts induced by execution errors, it is desirable to keep these errors as small as possible. Consequently, a rule of thumb that was developed for formation maneuver design was that no burn smaller than 0.05 m/s would be deemed acceptable. Shifting formation size up to 8 km and then back to 7 km at the next maneuver set made the maneuvers slightly larger, so meeting this 0.5 m/s guideline and giving good controller performance.

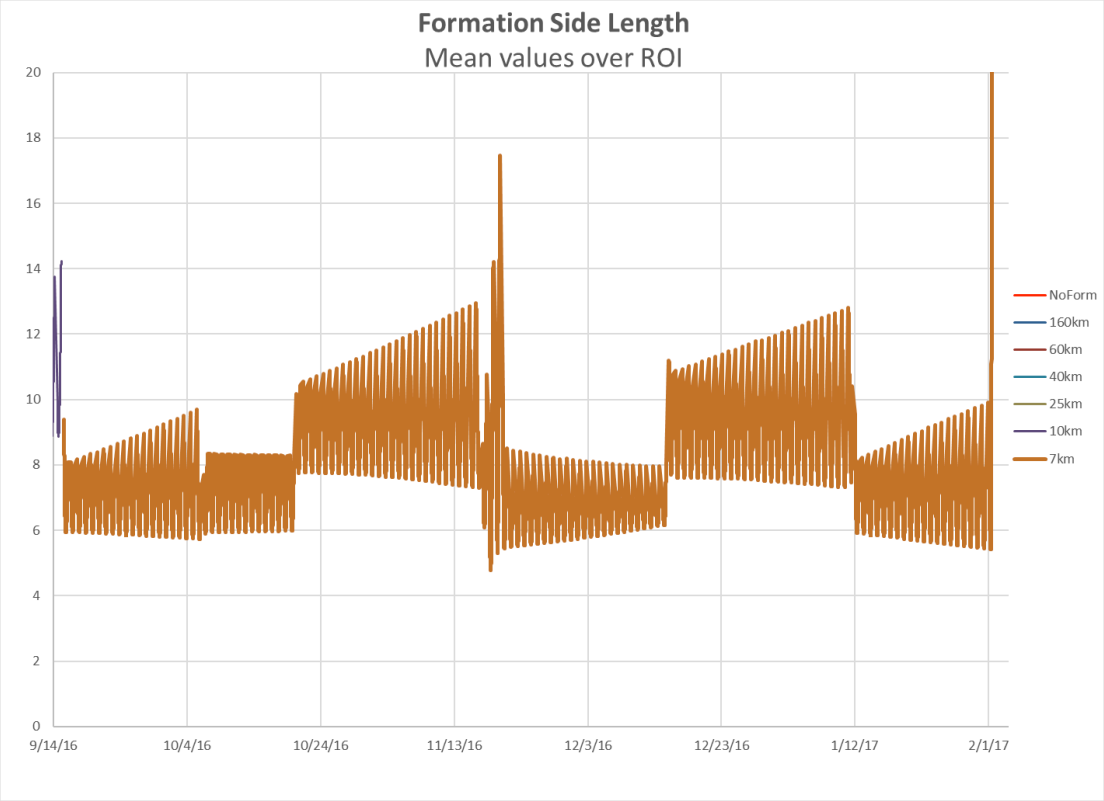

Figure 6. Evolution of Mean Sidelength, Phase 1b.

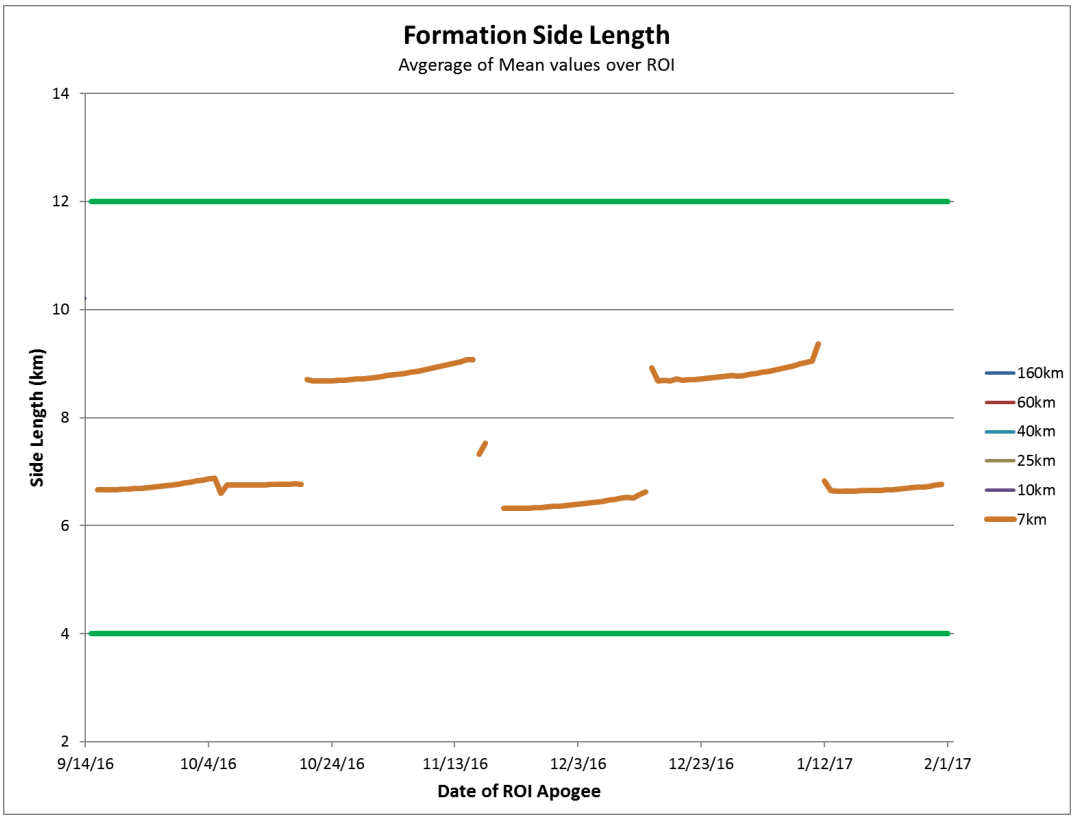

Figure 7. Evolution of Mean Sidelength Averaged Over RoI, Phase 1b.

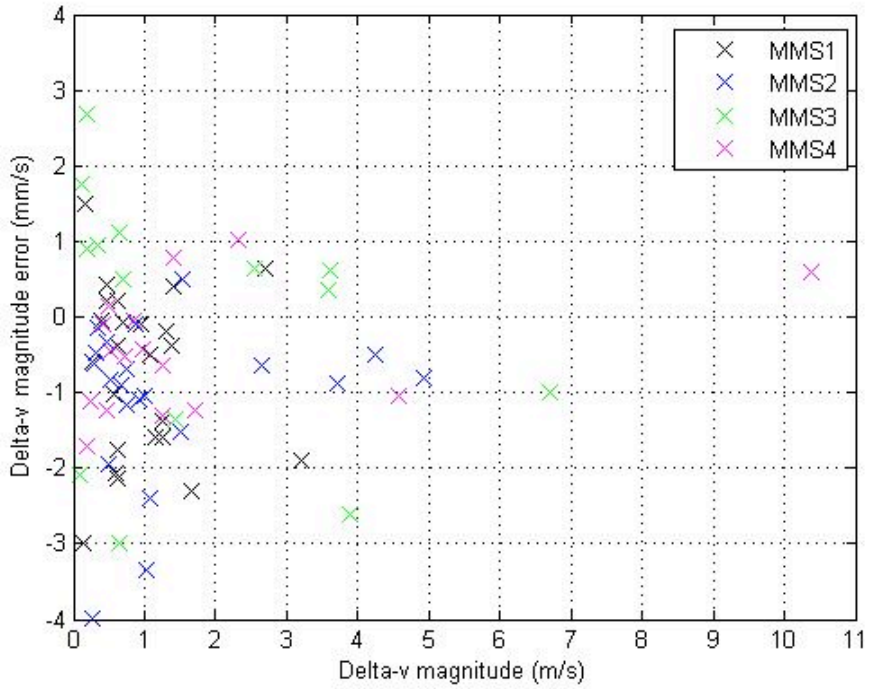

Figure 8. ΔV Execution Error (Magnitude).

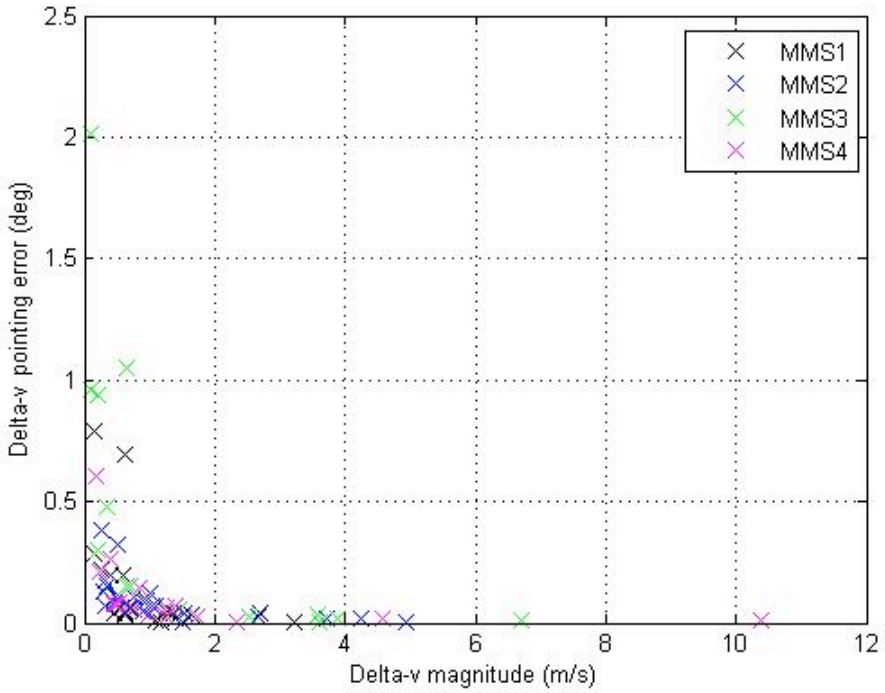

Figure 9. ΔV Execution Error (Direction).

A spike can be observed in Figure 6 around Nov. 18; a small line segment is also visible in Figure 7 on this same date. This is a result of a missed FM2 burn by MMS3 in a formation maneuver set: this caused

MMS3 to drift significantly out of position before being maneuvered back (using a procedure developed for a previous missed burn and described in Reference 4) a few days later. As part of this anomalous trajectory, there was a close approach between MMS3 and MMS2: see the companion paper Reference 7 for further details.

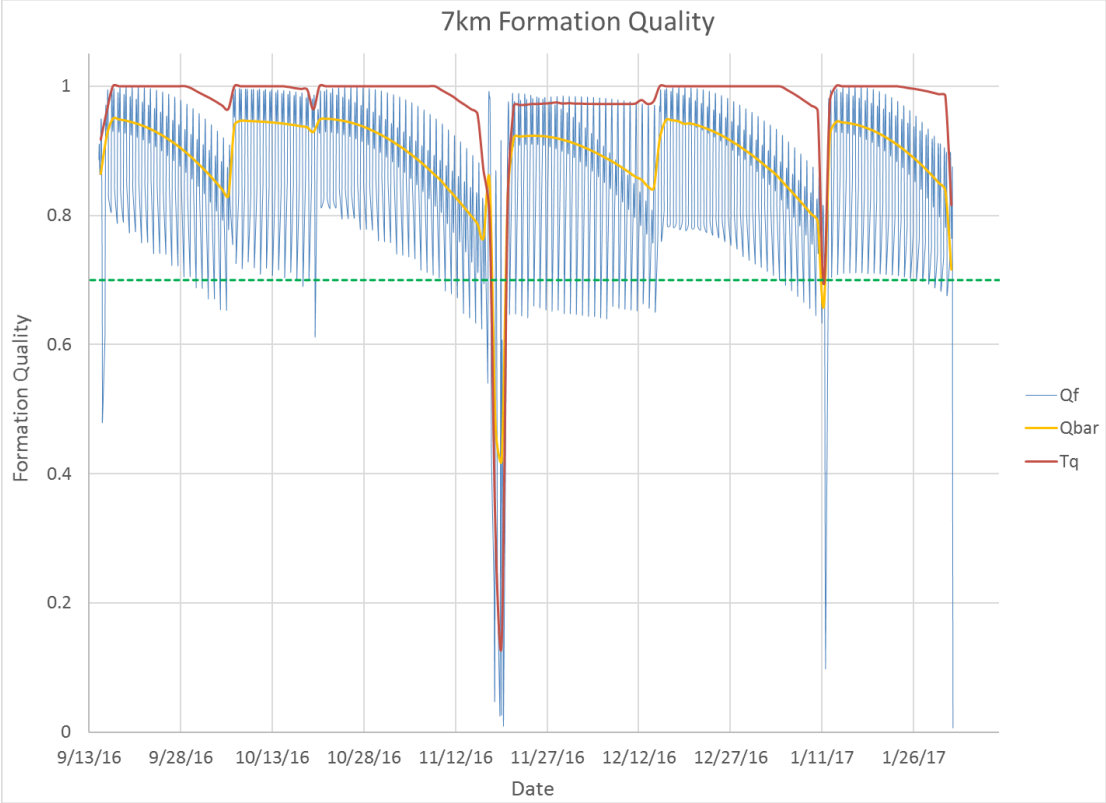

Figure 10. Evolution of Formation Quality Factor, Phase 1b.

Figure 10 shows the evolution of formation QF over Phase 1b. If a set of formation maneuvers is triggered because the formation has degraded to the point where its QF is no longer acceptable, it will occur before the quantity Tq hits the 0.7 limit. It can be seen that this threshold was hardly ever reached during Phase 1b: this is a result of the fact that most formation maneuvers were triggered not as a result of QF degradation, but rather in order to prevent an uncomfortably close pass between two spacecraft. The exception is the period immediately following the MMS3 missed burn on Nov. 18: over the several days before this spacecraft could be maneuvered to rejoin the others, the formation was severely affected and so had a very low QF.

Finally, Figure 11 shows the remaining fuel mass on each spacecraft from launch to one week into Phase 2a (see the second column of Table 1 for the orbit numbers corresponding to each maneuver). The large intial decrease corresponds to the five perigee-raise maneuvers that each spacecraft had to carry out shortly after launch; the largest remaining maneuvers are Formation Initialization (FI) and the various Formation Resizes (FRs). An attempt has been made to balance the fuel remaining on each spacecraft by judicious selection of the reference spacecraft for each set of formation maneuvers: it can be seen that this goal was closely achieved by the time of the start of Phase 2a.

Maintaining a given formation size is relatively inexpensive in terms of fuel: excluding the initial relatively large resize maneuvers, the average consumption rate is around 0.8 kg/month per MMS. The rate is reduced even further for the small formations of Phase 1b. This results from the fact that, although

small formations typically require somewhat more frequent maneuvers than do larger ones, the sizes of the burns are small, leading to a reduced rate of fuel consumption.

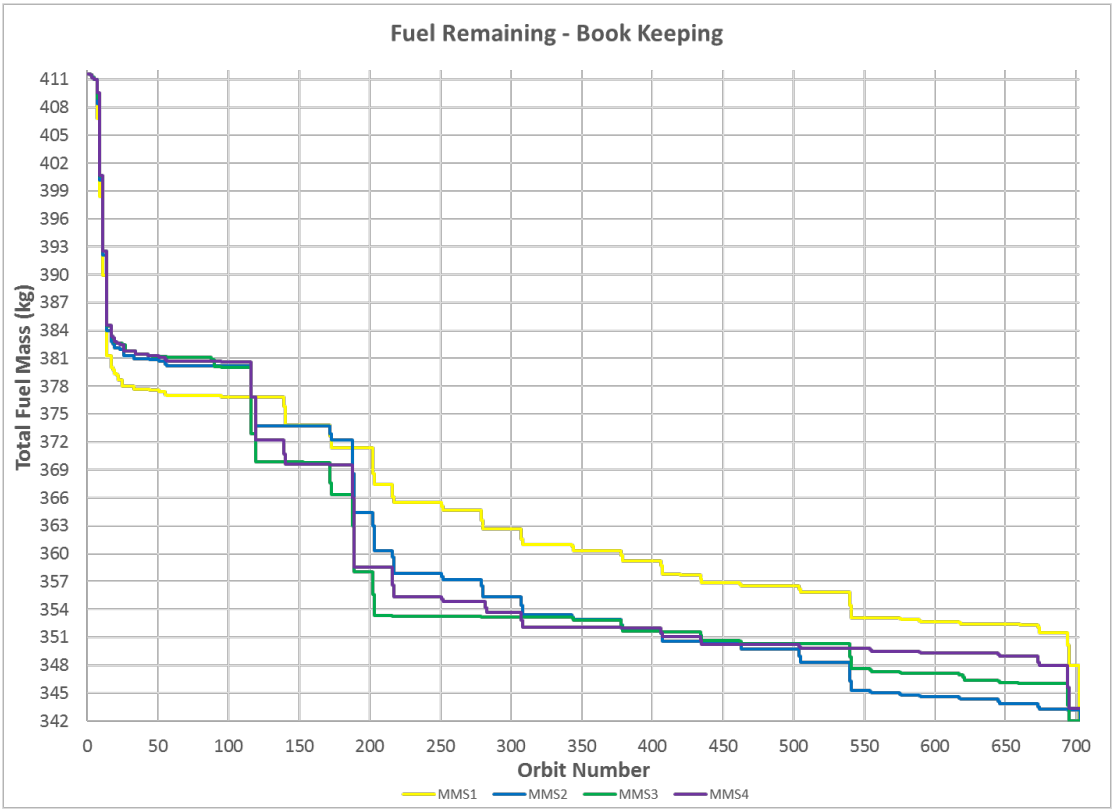

Figure 11. Fuel Remaining per Spacecraft, Launch to Phase 2a.

TRIM BURN

It has often been found while flying at small formation sizes in Phase 1b that one particular spacecraft pair (typically MMS1 and MMS4) often drifted slowly towards each other. The resulting danger of a conjunction then required that a Formation Maintenance (FM) maneuver set be carried out in order to "reset" the formation. In several cases, this had to be done earlier than originally planned, which led to disruption to science collection (since FM maneuvers occur in the science RoI) and additional fuel use. The underlying reason for this inter-satellite drift is that execution errors in the preceding FM set led to the semi-major axes of the MMS1 and MMS4 orbits being somewhat different, leading to different orbital periods and hence a slow drift rate.

The trim burn was designed during the Phase 1b small formation flight period in order to avoid this difficulty. This is a single burn by one of the spacecraft in the drifting pair, and is designed to reduce (ideally, null) the SMA difference between it and the other drifting MMS. Burns to change SMA are typically applied along the orbital velocity vector, as this is the most efficient direction. However, the SMA difference to be corrected in the trim case was typically small, on the order of 10 m, and the required burn size to correct this with a burn along the velocity would be too small to be feasible. In particular, it would be well below the 0.05 m/s maneuver lower limit imposed when using the MMS closed-loop Delta-v controller. Consequently, the trim burn uses the MMS open-loop "Checkout Mode" to apply a small Δv along the spin axis of the spacecraft, using a pair of 4.5 N (1 lbf) axial thrusters. Rather than commanding a desired Δv vector in Checkout Mode, the input that is uploaded to the spacecraft is the desired burn duration of the thrusters.

A limitation of Checkout Mode is that it does not make use of the rotational phasing of the spacecraft. For this reason, this mode cannot be used to apply a Δv with a component along a specified inertial direction in the MMS spin plane. This led to the decision to thrust only along the spin axis. So long as this vector is not perpendicular to the orbital velocity vector (which only occurs twice per orbit), there is a component of Δv along the orbital velocity vector, and consequently the desired small change in SMA can be produced.

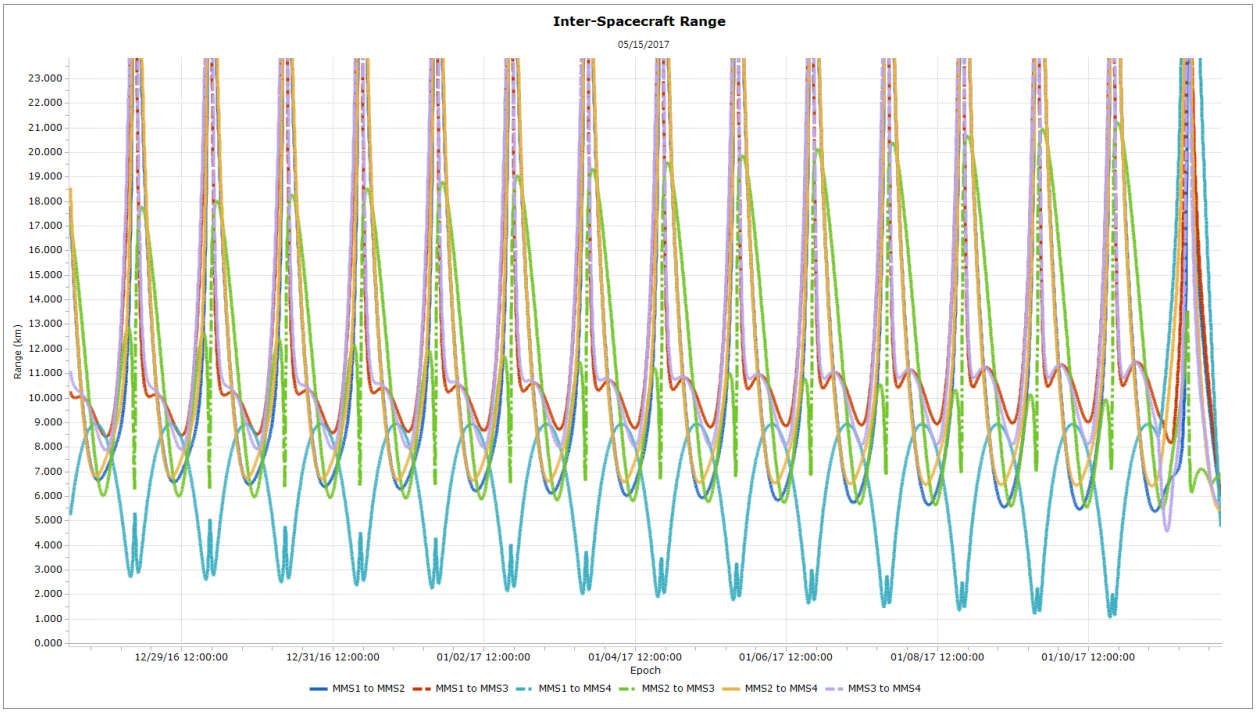

Figure 12. Evolution of ISRs, no MMS1 Trim.

Following design, development and testing, the trim burn was ready for application during the latter portion of Phase 1b. The opportunity arose following an FM set of maneuvers that took place in mid-Dec., 2016. Figure 12 shows the inter-satellite ranges (ISRs) between the 6 MMS pairs: it can be seen that the MMS1/MMS4 pair have a closing drift rate. This drift would have necessitated bringing forward the next formation maintenance maneuvers, which would not have been consistent with the desired Feb. 1-2, 2017 time of the Phase 2a resize to 60 km. Introducing a trim burn on Dec. 28 was a more attractive option, and had the additional benefit of providing a demonstration of this new type of maneuver.

Figure 13 shows the semi-major axes of the four MMSs before the application of the trim. It can be seen that the SMA difference between MMS1 and MMS4 was 10 m: the goal of the trim, to be carried out by MMS1, was to zero out this difference. Note that the SMA differences between, for instance, MMS2 and MMS3, although large, can be seen from Figure 12 not to lead to appreciable drift between these spacecraft. This is a consequence of where on the orbit the spacecraft pass closest: for MMS2/MMS3 this occurs near apogee (relatively insensitive to SMA differences), whereas for MMS1/MMS4 it is on the descending flank, near perigee (more sensitive). Consequently, the focus of the trim was only on nulling the SMA difference between MMS1 and MMS4.

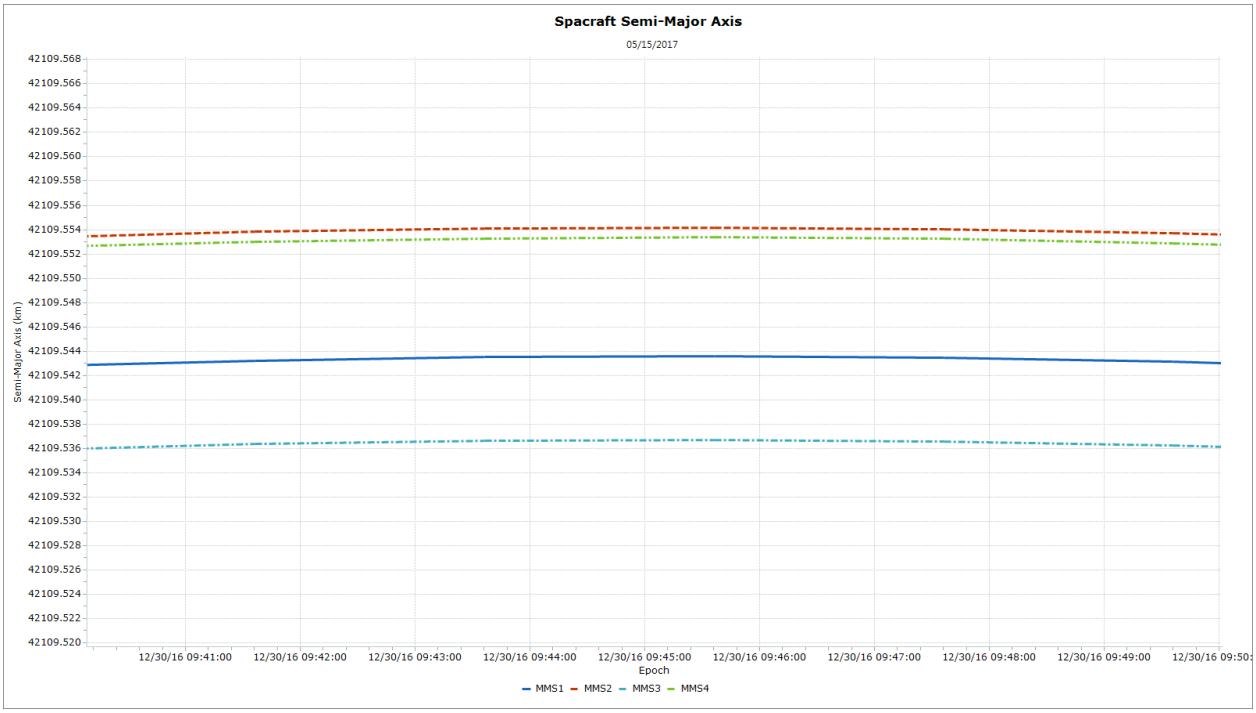

Figure 13. SMAs, no MMS1 Trim.

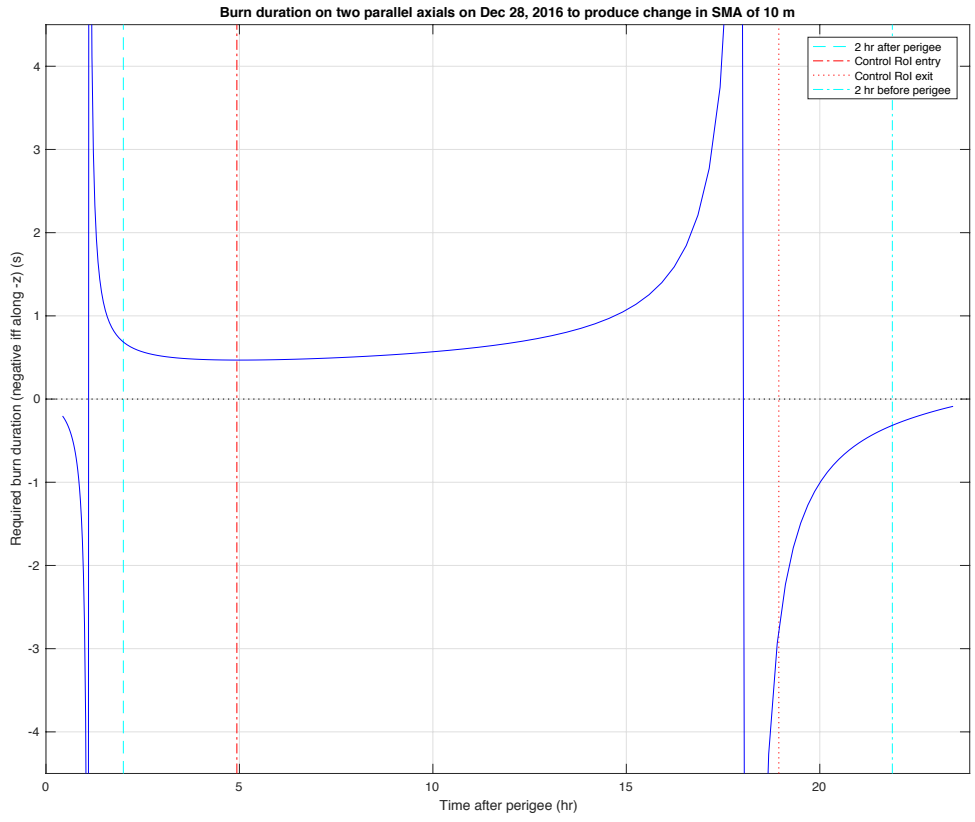

Figure 14. Effect of Trim Burn Location on Required Burn Duration.

Figure 14 plots the burn duration that is required to produce an SMA change of 10 m as a function of where on the orbit the trim is applied. The two spikes occur at the points on the orbit where the MMS spin axis is perpendicular to the orbital velocity vector. Also shown are the Region of Interest (central section between the two vertical red lines), and the interval in the vicinity of perigee: all of these should ideally be avoided, in order not to disrupt science or TDRS contact operations. The result of study of this plot was that the trim was designed as a 0.8 s burn to be applied 21 hours after perigee.

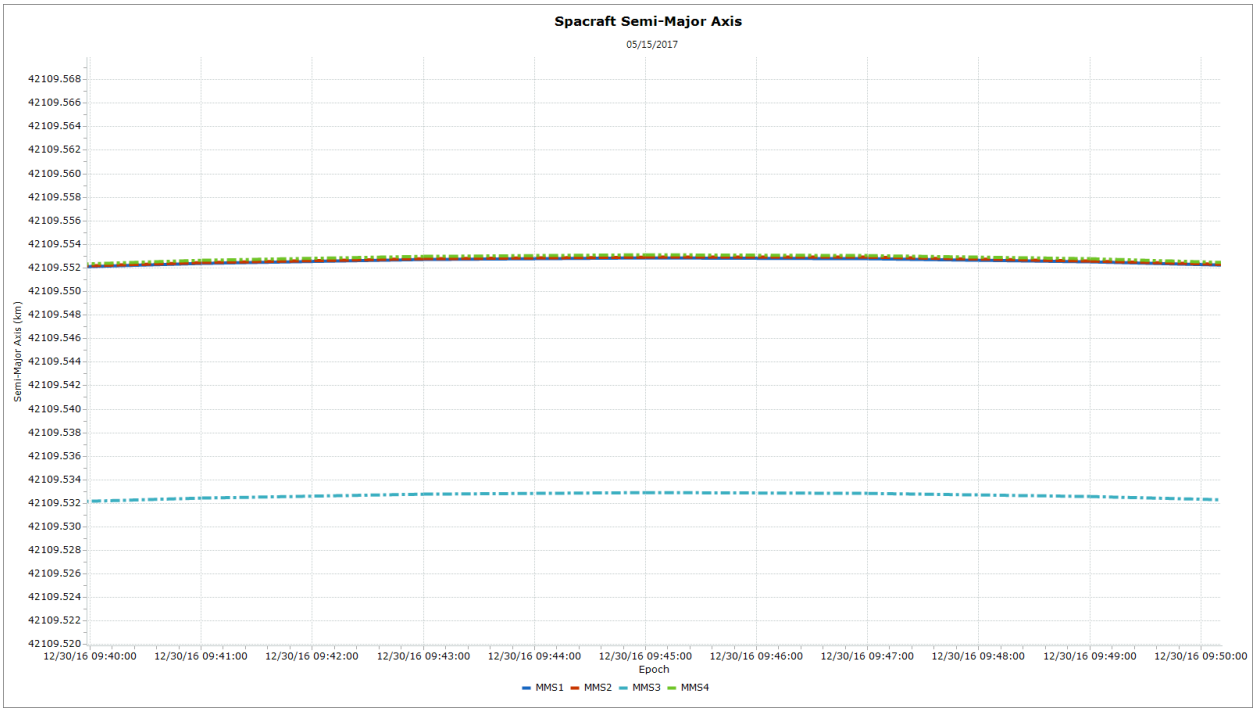

Figure 15. SMAs After MMS1 Trim.

The trim burn was carried out on Dec. 28, 2016, and was very accurate at nulling the 10 m SMA difference between MMS1 and MMS4, as can be seen from Figure 15. This accuracy confirms that the actual force applied by the axial thrusters was very close to the predicted value: in this sense, the trim burn also functioned as a calibration maneuver. Figure 16 then gives the resulting post-trim ISRs: it can be seen that there is an essentially zero drift rate between MMS1 and MMS4. This allowed the timing of the next FM maneuver set to be held as originally planned, meshing with the scheduled start of Phase 2a.

A final point concerning the trim burn is that the total fuel consumption was extremely modest: approximately 2.7 grams, as opposed to on the order of 0.2 kg per spacecraft for a typical FM set. In addition, performing a single burn on one spacecraft, rather than two burns on each of three as in a regular FM set, is a considerable operational simplification. It is likely that the trim will be a useful tool for any future flight in small formations. It is also a possible collision avoidance maneuver, as described in Reference 7.

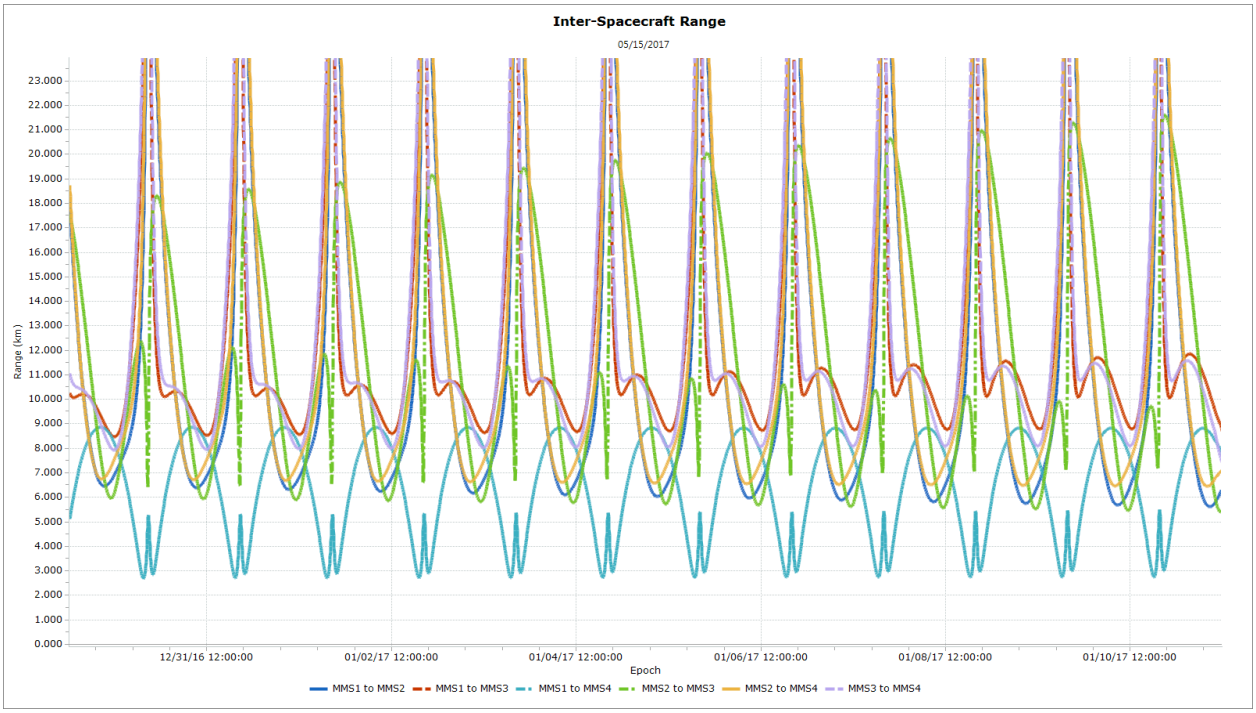

Figure 16. Evolution of ISRs After MMS1 Trim.

CONCLUSIONS

This paper described the underlying dynamics and findings of formation flying in the Magnetospheric Multiscale mission during Phase 1. The results demonstrate that MMS has been able to carry out formation flying while exceeding requirements for maneuver execution error and maneuver cadence. These results inspired the science team to request the investigation of evaluating the feasibility of flying formations smaller than 10 km and in return provide significantly enhanced science data. This was achieved during Phase 1b, which was flown essentially in its entirety at the reduced scale size of 7 km.

ACKNOWLEDGMENTS

The authors wish to acknowledge the invaluable contributions of the other members of the MMS Flight Dynamics team.

REFERENCES

[1] A.S. Sharma and S.A. Curtis, "Magnetospheric Multiscale Mission", *Nonequilibrium Phenomena in Plasmas*, Astrophysics and Space Science Library Vol. 321, Springer-Netherlands. pp. 179–195, 2005.

[2] T. Williams, “Launch Window Analysis for the Magnetospheric Multiscale Mission”, Paper AAS12-255, AAS/AIAA Space Flight Mechanics Meeting, Charleston, SC, Jan./Feb. 2013.

[3] D.H. Fairfield, “A Statistical Determination of the Shape and Position of the Geomagnetic Neutral Sheet”, *J. Geophysical Research*, Vol. 85, No. A2, pp. 775-780, Feb. 1980.

[4] T. Williams, N. Ottenstein, E. Palmer and M. Farahmand, “Initial Satellite Formation Flight Results from the Magnetospheric Multiscale Mission”, Paper AIAA 2016-5505, AIAA SPACE-2016, Long Beach, CA, Sept. 2016.

[5] D.J. Chai, S.Z. Queen and S.J. Placanica, "Precision Closed-Loop Orbital Maneuvering System Design and Performance for the Magnetospheric Multiscale Formation", Paper 181, 25th International Symposium on Space Flight Dynamics, Munich, Germany, Oct. 2015.

[6] A. Long, M. Farahmand and J.R. Carpenter, "Navigation Operations for the Magnetospheric Multiscale Mission", Paper 015, 25th International Symposium on Space Flight Dynamics, Munich, Germany, Oct. 2015.

[7] T. Williams, N. Ottenstein, E. Palmer and D. Godine, "Conjunction Assessment Techniques and Operational Results from the Magnetospheric Multiscale Mission", 9th International Workshop on Satellite Constellations and Formation Flying, Boulder, CO, June 2017.

[8] S.P. Hughes, "Formation Design and Sensitivity Analysis for the Magnetospheric Multiscale Mission (MMS)", Paper AIAA 2008-7357, *Proc. AIAA/AAS Astrodynamics Specialist Conference*, Honolulu, HI, Aug. 2008.